Published in final edited form as:
J Infect Dis. 2009 July 15; 200(2): . doi:10.1086/599795.

Dengue Virus Infection Differentially Regulates Endothelial Barrier Function over Time through Type I Interferon Effects

Ping Liu[a], **Marcia Woda**, **Francis A. Ennis**, and **Daniel H. Libraty**
Center for Infectious Disease and Vaccine Research, University of Massachusetts Medical School, Worcester

Abstract

Background—The morbidity and mortality resulting from dengue hemorrhagic fever (DHF) are largely caused by endothelial barrier dysfunction and a unique vascular leakage syndrome. The mechanisms that lead to the location and timing of vascular leakage in DHF are poorly understood. We hypothesized that direct viral effects on endothelial responsiveness to inflammatory and angiogenesis mediators can explain the DHF vascular leakage syndrome.

Methods—We used an in vitro model of human endothelium to study the combined effects of dengue virus (DENV) type 2 (DENV2) infection and inflammatory mediators on paracellular macromolecule permeability over time.

Results—Over the initial 72 h after infection, DENV2 suppressed tumor necrosis factor (TNF)–α–mediated hyperpermeability in human umbilical vein endothelial cell (HUVEC) monolayers. This suppressive effect was mediated by type I interferon (IFN). By 1 week, TNF-α stimulation of DENV2-infected HUVECs synergistically increased cell cycling, angiogenic changes, and macromolecule permeability. This late effect could be prevented by the addition of exogenous type I IFN.

Conclusions—DENV infection of primary human endothelial cells differentially modulates TNF-α–driven angiogenesis and hyperpermeability over time. Type I IFN plays a central role in this process. Our findings suggest a rational model for the DHF vascular leakage syndrome.

Dengue is caused by infection with one of the dengue viruses (DENVs), a group of 4 antigenically related mosquito-borne flaviviruses [1]. Dengue is the most prevalent arboviral disease worldwide and produces significant morbidity and mortality throughout the tropics and subtropics [2]. DENV infections produce a wide spectrum of clinical illness, ranging from asymptomatic or mild illness to a severe and life-threatening disease—dengue hemorrhagic fever (DHF). The hallmark of DHF is vascular endothelial dysfunction manifested by a vascular leakage syndrome and sometimes a hemorrhagic diathesis. The morbidity and mortality of DHF are largely driven by the vascular leakage and its ensuing complications.

The mechanisms of endothelial barrier dysfunction that lead to the unique vascular leakage syndrome of DHF are poorly understood. The DENVs are not cytopathic to endothelial cells in vitro [3, 4]. Viral antigen–positive endothelial cells have been seen in autopsy tissues with

Reprints or correspondence: Dr. Daniel H. Libraty, Rm. S6-862, CIDVR, UMMS, 55 Lake Ave. N., Worcester, MA 01655 (daniel.libraty@umassmed.edu)..
[a]Present affiliation: Genzyme Corporation, Framingham, Massachusetts.

Potential conflicts of interest: none reported.

Presented in part: American Society of Tropical Medicine and Hygiene 56th Annual Meeting, Philadelphia, 4–8 November 2007.

minimal or no endothelial destruction [5, 6]. Plasma leakage develops abruptly during viral clearance and early symptom recovery, at a time of significant immune activation [7]. The initial plasma leakage is focal and occurs predominantly in the pleural and peritoneal spaces [8]. The prevailing explanation for vascular leakage in DHF is that immune responses to DENV infection produce a cytokine storm that leads to the transient compromise of endothelial barrier function [7]. Many proinflammatory cytokines, angiogenesis factors, and other mediators (e.g., thrombin, metalloproteinases, and prostaglandins) can decrease endothelial barrier function and thereby increase vascular permeability [9]. Circulating levels of many vascular permeability mediators are indeed elevated in patients with DHF [7, 10-12] and can be produced by DENV-infected cells in vitro [13, 14]. However, increased levels of these soluble mediators are also present in other diverse inflammatory conditions, such as bacterial sepsis [15], cerebral malaria [16], autoimmune diseases [17], and malignancies [18]. The vascular leakage characteristics of these varied conditions are distinct from those of DHF.

We hypothesized that direct viral effects on the responsiveness of endothelium to inflammatory and angiogenesis mediators are responsible for the vascular leakage characteristics of DHF. We found that DENV type 2 (DENV2) infection could suppress tumor necrosis factor (TNF)–α–mediated hyperpermeability in human umbilical vein endothelial cell (HUVEC) monolayers. This suppressive effect was seen up to 72 h after DENV2 infection. However, 1 week after infection TNF-α–mediated hyperpermeability was enhanced in DENV2-infected endothelium, compared with that in uninfected endothelium. The present study elucidates the critical role played by DENV and TNF-α–induced type I interferon (IFN) in the modulation of endothelial barrier function over time. Our results provide the foundation for a rational model of vascular leakage in DHF and potential therapeutic approaches.

METHODS

Reagents

Reagents used were recombinant (r) TNF-α (Invitrogen), rIFN-γ (Biosource International), rIFN-β (PBL Laboratories), rB18R protein (eBioscience), and soluble vascular endothelial growth factor (VEGF) receptor 2 (VEGFR2; R&D Systems).

Viruses and cells

DENV2 strain 16681 was propagated in the mosquito cell line C636, and virus stocks were titered by limiting-dilution plaque assay on Vero cells. Virus stocks were free of endotoxin and *Mycoplasma* contamination. In some experiments, DENV2 was inactivated by means of ultraviolet light (254-nm ultraviolet A light at 2300 μW/cm^2 for 15 min on ice). Primary HUVECs were cultured in EGM-2 medium supplemented with EGM-2MV SingleQuots (Lonza). All experiments were performed with subculture 2 cells.

Macromolecule paracellular permeability assays

Assays were performed using modifications of a protocol that has been described elsewhere [19]. Briefly, HUVECs were plated at 1×10^5 cells/well on collagen-coated transwell inserts (0.4-μm-pore, 6.5-mm-diameter Transwell-COL; Costar). After 1–2 days, the HUVECs formed a confluent monolayer and were infected with DENV2 or mock control (C636 culture supernatant). Virus or C636 supernatant was added to the top chamber, adsorbed for 2 h at 37°C, and washed, and fresh medium was added. Cytokines and soluble mediators were added at the indicated concentrations to the top and bottom chambers. rTNF-α or rIFN-γ was added to the HUVEC cultures 18 h before measurement of macromolecule paracellular permeability.

Paracellular permeability was measured by the addition of 500 μg/mL fluorescein isothiocyanate–conjugated 70-kDa dextran (Invitrogen) to the top chamber. Fluorescence in the bottom chamber was read after 15, 30, and 60 min at 37°C, and assays were performed in quadruplicate. In this transwell system, endothelial monolayer permeability is directly proportional to the flux of 70-kDa dextran across the monolayer. This was expressed mathematically as the first derivative (dC/dt) of the plot of concentration *(C)* versus time *(t)* (SigmaPlot, version 9.0; Systat).

Gene expression microarrays

Total cellular RNA from HUVECs was isolated using the RNeasy Kit (Qiagen). Equal amounts of cellular RNA from 4 replicate experiments were pooled together for each condition, labeled with biotin, and then hybridized to human oligonucleotide microarrays (Affymetrix HG-Focus), as described elsewhere [20]. Signal values from each of the 8793 probe sets were calculated by robust multiarray analysis [21] in GeneSpring GX software (Agilent Technologies). Samples were normalized against the day 7 mock-infected condition by dividing each measurement for each gene in all test samples by that gene's measurement in the control sample. Expression levels were organized by hierarchical cluster analysis using a Pearson metric. Affymetrix gene identification numbers for IFN-inducible genes were obtained from the supplemental information of Indraccolo et al. [22] and were imported into GeneSpring. Gene ontology analysis was performed at the DAVID (Database for Annotation, Visualization and Integrated Discovery) Web site (http://david.abcc.ncifcrf.gov) [23] to obtain functional annotation charts. Selection criteria were a count of at least 5 genes in the list, $P < .003$ represented in the gene ontology category, a fold enrichment of at least 1.5, and a gene ontology category size <300 genes.

Quantitative reverse-transcription polymerase chain reaction (qRT-PCR) and enzyme-linked immunosorbent assay (ELISA)

qRT-PCR for IFN-β, Toll-like receptor (TLR) 3, retinoic acid–inducible gene (RIG) 1, and β2-microglobulin was performed on an ABI 7300 real-time PCR machine, using TaqMan reagents and a standard protocol (Applied Biosystems). qRT-PCR for type I IFN–stimulated genes (ISGs) was performed by the Transcriptome Fingerprinting Core at the Mount Sinai School of Medicine (New York, New York), using a protocol that has been described elsewhere [24]. Each transcript in each sample was assayed in triplicate, and 3 house-keeping genes (β-actin, Rps11, and tubulin genes) were used for global normalization [25]. Levels of IFN-β in cell culture supernatants were measured by ELISA, in accordance with the manufacturer's instructions (Biosource International).

Cell cycle and apoptosis analysis

Adherent and nonadherent HUVECs were washed with phosphate-buffered saline and fixed in 95% ice-cold ethanol for 24 h. Cells were pelleted, washed, and resuspended in phosphate-buffered saline containing 2 mmol/L $MgCl_2$, 50 μg/mL RNase A, and 50 μg/mL propidium iodide (Sigma). The stained cells were incubated for 20 min at 37°C and then analyzed on a FACSCalibur flow cytometer (BD Biosciences) equipped with pulse-processing electronics for doublet discrimination. The percentage of cells that were apoptotic or necrotic and the proportion of live cells in each of the cell cycle phases was determined using ModFit LT software (Verity Software House).

Immunohistochemical analysis

HUVECs were cultured to a confluent monolayer on 8-chamber tissue-culture treated glass slides (BD Biosciences). Infection with DENV2 strain 16681 was done as described above. At the indicated time points, virus-infected and uninfected cell culture slides were fixed in

−20°C methanol for 20 min and air dried. The slides were permeabilized, blocked, and incubated with anti–DENV E protein mouse monoclonal antibody 3H5-1 (American Type Culture Collection) or isotype control monoclonal antibody. Secondary antibody and immunoperoxidase staining were performed using the Vectastain ABC Kit and diaminobenzidine development (Vector Laboratories). The approximate percentage of viral antigen–containing cells was determined by counting at least 100 cells per chamber for 4 chambers and averaging the percentages of stained cells per total cells counted.

Scanning electron microscopy

HUVECs on collagen-coated transwell inserts were fixed by adding 0.1 mL of 2.5% (vol/vol) glutaraldehyde in 0.1 mol/L phosphate buffer (pH 7.0), followed by incubation at room temperature for 30 min. The samples were washed, fixed for 20 min in 1% osmium tetroxide, and left overnight at 4°C in fresh buffer (pH 7.0). The inserts were washed again in ultrapure water, dehydrated through a graded series of ethanol to 100%, and then critical-point dried in liquid CO_2. The dried cell culture inserts were mounted and carbon coated in a vacuum evaporator. Cells were examined using an Quanta 200F microscope (FEI) at 5.0–20.0 Kv. Intercellular-gap distances were determined by measuring 10–15 independent cell-cell distances in ×1000 magnification fields that spanned a 3 × 3 grid pattern over the fixed transwell inserts (Acronis True Image; FEI).

Statistical analysis

The SPSS software package (version 15.0) was used for statistical analyses. For normally distributed variables, comparisons between 2 groups were analyzed using Student's *t* test. For nonnormally distributed variables, comparisons between 2 groups were analyzed using the Mann-Whitney *U* test and the Kolmogorov-Smirnov *Z* test. Comparisons among multiple groups were performed using 1-way analysis of variance and post-hoc least significant difference tests.

RESULTS

Suppression of TNF-α-driven endothelial hyperpermeability by DENV2 soon after infection

rTNF-*α* increased the macromolecule permeability of HUVEC monolayers grown on collagen-coated transwell membranes in a dose-dependent manner. Seventy-two hours after DENV2 infection (multiplicity of infection [MOI], 0.5), TNF-*α*–mediated hyperpermeability was suppressed in virus-infected HUVEC monolayers, compared with that in mock-infected controls (figure 1*A*). There were no significant viral effects on endothelial barrier function in the absence of rTNF-*α*. The same findings were also obtained in HUVECs infected with DENV2 at an MOI of 4 (data not shown).

Enhancement of TNF-α-driven endothelium hyperpermeability by DENV2 within 1 week after infection

DHF is characterized by the onset of increased vascular permeability well beyond 72 h after the beginning of viremia [7]. We therefore compared the permeability characteristics of DENV2-infected and mock-infected HUVECs 1 week after infection. The percentage of DENV2 antigen–positive endothelial cells increased from ~10% to ~30% between days 3 and 7 after infection (MOI, 0.5). The permeability of HUVEC monolayers was only slightly increased 1 week after DENV2 infection alone. TNF-*α*–driven hyperpermeability across HUVEC monolayers was significantly augmented 7 days after DENV2 infection, compared with that in mock-infected controls (figure 1*B*). We focused our subsequent experiments on TNF-*α*, because it has inflammatory and angiogenic activities [26]. However, the

differential early and late viral effects on endothelium macromolecule permeability were not unique to rTNF-α stimulation and were also seen with rIFN-γ stimulation (data not shown).

DENV2-dependent early suppression of TNF-α–driven endothelial hyperpermeability mediated by type I IFN

The early suppressive effect of DENV2 infection on TNF-α–mediated endothelial hyperpermeability was dependent on live virus. Live DENV2 infection (MOI, 0.5) decreased rTNF-α–mediated (1 ng/mL) HUVEC monolayer macromolecule permeability to a mean ± standard error (SE) of 49% ± 2% of the mock-infected control values 72 h after infection ($n = 7$; $P = .02$). The permeability across ultraviolet light-inactivated DENV2-infected HUVECs was not significantly different from that for mock-infected controls (mean ± SE, 88% ± 14%; $n = 5$; $P = .7$). Live DENV2 induced IFN-β messenger RNA (mRNA) and protein expression from HUVECs soon after infection. Virus-induced IFN-β production was augmented by rTNF-α or rIFN-γ stimulation up to 2 days after infection (data not shown). Pretreatment of HUVECs with rIFN-β suppressed TNF-α–mediated endothelial hyperpermeability at 72 h (figure 2*A*). To inhibit DENV2- and TNF-α–induced IFN-β signaling, we used a recombinant vaccinia virus-encoded soluble type I IFN receptor antagonist protein (rB18R) [27]. The addition of rB18R to HUVEC monolayers after virus adsorption reversed the DENV2 suppressive effects on TNF-α–driven hyperpermeability (figure 2*B*). Our data demonstrate that DENV2 infection can ameliorate TNF-α–driven hyperpermeability through early type I IFN production and signaling.

Cessation of enhancement of ISG expression by TNF-α stimulation 1 week after DENV2 infection

We measured the expression of ISGs (*IFIT1*, *ISG54*, *MX1*, *CXCL10*, and *RIG1*) in DENV2-infected HUVECs that had or had not been stimulated overnight with rTNF-α on days 2, 5, and 7 after infection. ISG mRNA levels increased moderately over time in DENV2-infected HUVECs. TNF-α stimulation soon after DENV2 infection (day 2) enhanced the virus-induced expression of these ISGs. This enhancing effect disappeared when TNF-α stimulation occurred at the later time points (figure 3).

Enhancement of endothelial cell cycling by TNF-α stimulation 1 week after DENV2 infection

We next identified 2 gene clusters differentially expressed in rTNF-α–stimulated HUVECs between days 3 and 7 after DENV2 infection. When TNF-α–driven hyperpermeability was suppressed by DENV2 infection (day 3), the expression of genes involved in cell cycling and growth was down-regulated and that of genes involved in microtubule assembly regulation was up-regulated, compared with control values. When TNF-α–driven hyperpermeability was augmented by DENV2 infection (day 7), these gene expression patterns were reversed—cell cycling and growth genes were up-regulated, and microtubule assembly genes were down-regulated (figure 4).

We directly measured the effects of DENV2 infection and TNF-α stimulation on cell cycling and cell death by propidium iodide staining of HUVEC DNA content. The percentage of apoptotic or necrotic HUVECs in mock-infected cell cultures increased from a mean ± SE of 5% ± 3% on day 3 to 21% ± 6% on day 7 ($n = 4$; $P = .08$). There were no significant differences in the frequency of apoptotic or necrotic cells among the mock infection, DENV2 infection, TNF-α stimulation, and DENV2 infection plus TNF-α stimulation conditions at each time point. There were no significant differences in the proportion of endothelial cells moving from G_0/G_1 to the S or G_2/M cell cycle phases on day 3 (figure 5*A*). TNF-α stimulation significantly increased the proportion of DENV2-infected HU-VECs moving from G_0/G_1 to S or G_2/M on day 7, compared with that for DENV2

infection or TNF-α stimulation alone. This augmented cell cycle progression could be reversed by the addition of rIFN-β 5 days after DENV2 infection and before TNF-α stimulation (figure 5*B*).

Promotion of angiogenic changes in the endothelial cell monolayer by TNF-α stimulation 1 week after DENV2 infection

Cell cycle control is critically linked to endothelial morphological changes and barrier dysfunction [28, 29]. DENV2-infected HUVECs had a typical rhomboid shape and adhered tightly to collagen-coated transwell membranes 3 and 7 days after infection (figure 6*A* and 6*B*). As expected, rTNF-α–stimulated HUVECs became large and elongated but by and large remained adherent to the underlying extracellular matrix (figure 6*C*) [30]. The same morphology was also seen in the day 3 DENV2-infected plus rTNF-α–stimulated HUVECs (figure 6*D*). In day 7 DENV2-infected plus rTNF-α–stimulated HUVECs, there was more prominent contraction and detachment of large and elongated endothelial cells (figure 6*E* and 6*F*). As such, the intercellular-gap distances were greatest in the day 7 DENV2-infected plus rTNF-α-stimulated HUVEC monolayers (median ± standard deviation, 8.24 ± 10.7 μm for DENV2 infection plus rTNF-α stimulation [$P < .001$ for the comparisons with mock infection and DENV2 infection, and $P = .02$ for the comparison with rTNF-α stimulation], 4.4 ± 6.4 μm for rTNF-α stimulation [$P = .01$ for the comparison with mock infection], 1.9 ± 2.1 μm for DENV2 infection, and 2.9 ± 4.2 μm for mock infection). These phenomena are seen in the early steps of angiogenesis and are mediated by multiple and complex interacting signals [31-33]. VEGF is a prototypical angiogenesis mediator. Inhibition of extracellular VEGF signaling by soluble VEGFR2 did not significantly decrease macromolecule permeability across day 7 DENV2-infected plus rTNF-α-stimulated HUVECs (data not shown). Doxycycline, an inhibitor of matrix metalloproteinases and VEGF-driven angiogenesis [34], also had no significant effect. However, rIFN-β was able to ameliorate the increase in macromolecule permeability, as it had ameliorated the increase in cell cycle progression (figure 7).

DISCUSSION

DHF is characterized by a unique vascular leakage syndrome. Many inflammatory and angiogenesis mediators increase vascular permeability to plasma proteins in venular and capillary endothelium [9, 35]. The prevailing model of the pathogenesis of DHF has simply attributed the vascular leakage syndrome to induction of 1 or more of these permeability-increasing mediators. This paradigm alone does not satisfactorily explain important and distinguishing characteristics of vascular leakage in DHF. We propose that vascular leakage in DHF can be better explained by a differential response of virus-infected endothelium over time to inflammatory and angiogenesis mediators.

We have demonstrated that DENV2-infected endothelial cells exposed to TNF-α soon after infection increased type I IFN production and signaling, compared with that for DENV2 infection alone. This early type I IFN ameliorated TNF-α–driven (and IFN-γ–driven) hyperpermeability up to 3 days after DENV2 infection. By 1 week after DENV2 infection, TNF-α no longer augmented type I IFN signaling, and TNF-α–driven endothelial hyperpermeability was enhanced. DENV2 infection and TNF-α synergized to augment endothelial cell cycle progression and the morphological changes of early angiogenesis. Addition of exogenous rIFN-β at this later time point was able to ameliorate the increased cell cycling and macromolecule permeability.

The gross pathological findings in DHF are similar to those seen in many other viral hemorrhagic fevers [6]. Although vascular endothelium is not widely and massively infected, DENV infection of endothelial cells in lungs, spleen, and kidney has been seen in

autopsy tissues [5, 6, 36]. DENV infection produces vascular leakage primarily in the pleural and peritoneal spaces [8]. A notable limitation of the reported autopsy studies has been that vascular endothelial cells in pleural and peritoneal tissues have not been examined. We postulate that DENV infection of endothelial cells in these target tissues plays a key role in the vascular leakage syndrome of DHF.

The early innate cellular response in DENV-infected endothelial cells includes production of type I IFN. TLR3 and RIG1 mRNAs were present in HUVECs (data not shown) and may be involved in the virus-dependent stimulation of type I IFN production [37]. Early type I IFN production and ISG expression were enhanced in DENV2-infected HUVECs by TNF-α stimulation. This type I IFN suppressed TNF-α–driven hyperpermeability. Our findings are consistent with the clinical course of DHF. Vascular leakage is not seen over the first several days of viremia, despite an innate immune response that produces inflammatory and vascular permeability mediators [10, 11, 38, 39]. Minagar et al. [40] have also reported that type I IFN can inhibit IFN-γ–mediated vascular permeability. We postulate that early type I IFN production in DENV-infected endothelium counteracts the permeability-enhancing effects of common innate immune response cytokines and mediators.

Approximately 1 week after infection, type I IFN signaling and ISG expression in DENV-infected endothelial cells were no longer enhanced by TNF-α. The DENV-infected endothelial cells became hyperresponsive to the angiogenesis- and permeability-enhancing effects of TNF-α. We postulate that ISG expression induced by the combination of DENV infection and TNF-α decreased over time because of the accumulation of viral nonstructural proteins that inhibit type I IFN signal transduction and signal transducer and activator of transcription 1 function (NS4B, NS4A, and NS2A) [41]. Exogenous type I IFN added well after virus infection was able to prevent this increase in cell cycling and macromolecule permeability. Exogenous type I IFN likely overwhelmed the virus-mediated type I IFN signaling antagonism and exerted antiproliferative and antiangiogenesis effects [42, 43].

We used low-passaged primary HUVECs in order to develop a preliminary mechanistic model of vascular leakage in DHF [44]. The vascular endothelium within and among different organs is heterogeneous [45, 46], and, as previously noted, the organ-specific endothelial tropism of DENVs has not been well studied. The relatively undifferentiated HUVECs formed tight interendothelial junctions. However, interendothelial junction regulation may differ among heterogeneous organ-specific endothelia and is a potential limitation of our study. We also focused specifically on paracellular macromolecule (i.e., albumin) permeability by measuring the flux of 70-kDa dextran rather than relying on transendothelial electrical resistance measurements [9, 47]. Early classic studies demonstrated that increased vascular permeability to plasma proteins in inflammatory conditions occurs through paracellular pathways in venular and sometimes capillary endothelium [9, 48]. This does not exclude the possibility that perturbation of physiological transcellular pathways or the endothelial glycocalyx may also take place. Our results provide insights into the likely key mode of vascular leakage in DHF.

The majority of individuals with either a primary or secondary DENV infection never develop DHF. The relative risk of developing DHF is greater after a secondary DENV infection than after a primary one [7, 49]. We propose that type I IFN production and signaling are typically augmented in DENV-infected endothelium exposed to innate inflammatory mediators soon after infection. The augmented type I IFN response suppresses any significant vascular leakage in this time frame. Approximately 1 week after DENV infection, the type I IFN response in endothelial cells is no longer enhanced. In this preliminary model, viral and host factors that promote robust and prolonged type I IFN signaling in a DENV-infected endothelial microenvironment could mitigate plasma leakage,

whereas viral and host factors that limit endothelial type I IFN signaling could set the stage for plasma leakage. Inflammatory and angiogenesis mediators can then act on DENV-infected endothelium to augment angiogenic changes and macromolecule permeability. The latter scenario may be more likely to take place during secondary infections. Our data support that complex interactions between host immune responses and DENV-infected vascular endothelial cells can better explain the DHF vascular leakage syndrome than either factor alone. We plan to test and refine the preliminary model suggested by our data in future studies using organ-specific endothelial cells isolated from pleural and peritoneal tissues. Our findings also continue to provide evidence that pharmacological type I IFN preparations that provide rapid and sustained therapeutic levels could be used to ameliorate the severity of dengue disease and prevent DHF [50]. An accurate mechanistic understanding of vascular leakage in DHF will lead to better therapeutic and preventive approaches.

Acknowledgments

We gratefully acknowledge the assistance of Gregory Hendricks for scanning electron microscopy, Kathy J. Martin for gene microarray analysis and figure preparation, and Sunil Shaw and Irene Bosch for their assistance in the permeability assays.

Financial support: National Institutes of Health (grant U19 AI57319).

The contents of this publication are solely the responsibility of the authors and do not necessarily represent the official views of the National Institutes of Health.

References

1. Henchal EA, Putnak JR. The dengue viruses. Clin Microbiol Rev. 1990; 3:376–96. [PubMed: 2224837]
2. Pinheiro FP, Corber SJ. Global situation of dengue and dengue haemorrhagic fever, and its emergence in the Americas. World Health Stat Q. 1997; 50:161–9. [PubMed: 9477544]
3. Dewi BE, Takasaki T, Kurane I. In vitro assessment of human endothelial cell permeability: effects of inflammatory cytokines and dengue virus infection. J Virol Methods. 2004; 121:171–80. [PubMed: 15381354]
4. Talavera D, Castillo AM, Dominguez MC, Gutierrez AE, Meza I. IL8 release, tight junction and cytoskeleton dynamic reorganization conducive to permeability increase are induced by dengue virus infection of microvascular endothelial monolayers. J Gen Virol. 2004; 85:1801–13. [PubMed: 15218164]
5. Jessie K, Fong MY, Devi S, Lam SK, Wong KT. Localization of dengue virus in naturally infected human tissues, by immunohistochemistry and in situ hybridization. J Infect Dis. 2004; 189:1411–8. [PubMed: 15073678]
6. Gubler, DJ.; Zaki, SR. Dengue and other viral hemorrhagic fevers. In: Nelson, AM.; Horsburgh, CR., Jr, editors. Pathology of emerging infections. Vol. 2. American Society for Microbiology; Washington, DC: 1998. p. 43-67.
7. Rothman AL, Ennis FA. Immunopathogenesis of dengue hemorrhagic fever. Virology. 1999; 257:1–6. [PubMed: 10208914]
8. World Health Organization. Dengue haemorrhagic fever: diagnosis, treatment, prevention and control. 2nd ed.. World Health Organization; Geneva: 1997.
9. Mehta D, Malik AB. Signaling mechanisms regulating endothelial permeability. Physiol Rev. 2006; 86:279–367. [PubMed: 16371600]
10. Libraty DH, Endy TP, Houng HS, et al. Differing influences of virus burden and immune activation on disease severity in secondary dengue-3 virus infections. J Infect Dis. 2002; 185:1213–21. [PubMed: 12001037]

11. Green S, Vaughn DW, Kalayanarooj S, et al. Early immune activation in acute dengue illness is related to development of plasma leakage and disease severity. J Infect Dis. 1999; 179:755–62. [PubMed: 10068569]
12. Sosothikul D, Seksarn P, Pongsewalak S, Thisyakorn U, Lusher J. Activation of endothelial cells, coagulation and fibrinolysis in children with dengue virus infection. Thromb Haemost. 2007; 97:627–34. [PubMed: 17393026]
13. Luplertlop N, Misse D, Bray D, et al. Dengue-virus-infected dendritic cells trigger vascular leakage through metalloproteinase overproduction. EMBO Rep. 2006; 7:1176–81. [PubMed: 17028575]
14. Libraty DH, Pichyangkul S, Ajariyakhajorn C, Endy TP, Ennis FA. Human dendritic cells are activated by dengue virus infection: enhancement by gamma interferon and implications for disease pathogenesis. J Virol. 2001; 75:3501–8. [PubMed: 11264339]
15. Cohen J. The immunopathogenesis of sepsis. Nature. 2002; 420:885–91. [PubMed: 12490963]
16. Hunt NH, Golenser J, Chan-Ling T, et al. Immunopathogenesis of cerebral malaria. Int J Parasitol. 2006; 36:569–82. [PubMed: 16678181]
17. Gutcher I, Becher B. APC-derived cytokines and T cell polarization in autoimmune inflammation. J Clin Invest. 2007; 117:1119–27. [PubMed: 17476341]
18. Lin WW, Karin M. A cytokine-mediated link between innate immunity, inflammation, and cancer. J Clin Invest. 2007; 117:1175–83. [PubMed: 17476347]
19. Shaw SK, Bamba PS, Perkins BN, Luscinskas FW. Real-time imaging of vascular endothelial-cadherin during leukocyte transmigration across endothelium. J Immunol. 2001; 167:2323–30. [PubMed: 11490021]
20. Warke RV, Xhaja K, Martin KJ, et al. Dengue virus induces novel changes in gene expression of human umbilical vein endothelial cells. J Virol. 2003; 77:11822–32. [PubMed: 14557666]
21. Irizarry RA, Hobbs B, Collin F, et al. Exploration, normalization, and summaries of high density oligonucleotide array probe level data. Biostatistics. 2003; 4:249–64. [PubMed: 12925520]
22. Indraccolo S, Pfeffer U, Minuzzo S, et al. Identification of genes selectively regulated by IFNs in endothelial cells. J Immunol. 2007; 178:1122–35. [PubMed: 17202376]
23. Dennis G Jr, Sherman BT, Hosack DA, et al. DAVID: database for annotation, visualization, and integrated discovery. Genome Biol. 2003; 4:P3. [PubMed: 12734009]
24. Fernandez-Sesma A, Marukian S, Ebersole BJ, et al. Influenza virus evades innate and adaptive immunity via the NS1 protein. J Virol. 2006; 80:6295–304. [PubMed: 16775317]
25. Kislauskis EH, Zhu X, Singer RH. Beta-actin messenger RNA localization and protein synthesis augment cell motility. J Cell Biol. 1997; 136:1263–70. [PubMed: 9087442]
26. Tracey KJ, Vlassara H, Cerami A. Cachectin/tumour necrosis factor. Lancet. 1989; 1:1122–6. [PubMed: 2566060]
27. Colamonici OR, Domanski P, Sweitzer SM, Larner A, Buller RM. Vaccinia virus B18R gene encodes a type I interferon-binding protein that blocks interferon alpha transmembrane signaling. J Biol Chem. 1995; 270:15974–8. [PubMed: 7608155]
28. Qin G, Kishore R, Dolan CM, et al. Cell cycle regulator E2F1 modulates angiogenesis via p53-dependent transcriptional control of VEGF. Proc Natl Acad Sci U S A. 2006; 103:11015–20. [PubMed: 16835303]
29. Verin AD, Birukova A, Wang P, et al. Microtubule disassembly increases endothelial cell barrier dysfunction: role of MLC phosphorylation. Am J Physiol Lung Cell Mol Physiol. 2001; 281:L565–74. [PubMed: 11504682]
30. Brett J, Gerlach H, Nawroth P, Steinberg S, Godman G, Stern D. Tumor necrosis factor/cachectin increases permeability of endothelial cell monolayers by a mechanism involving regulatory G proteins. J Exp Med. 1989; 169:1977–91. [PubMed: 2499653]
31. Hirschberg RM, Sachtleben M, Plendl J. Electron microscopy of cultured angiogenic endothelial cells. Microsc Res Tech. 2005; 67:248–59. [PubMed: 16170819]
32. Folkman J. How is blood vessel growth regulated in normal and neoplastic tissue? G. H. A. Clowes memorial award lecture. Cancer Res. 1986; 46:467–73. [PubMed: 2416426]
33. Risau W. Mechanisms of angiogenesis. Nature. 1997; 386:671–4. [PubMed: 9109485]

34. Fainaru O, Adini I, Benny O, et al. Doxycycline induces membrane expression of VE-cadherin on endothelial cells and prevents vascular hyperpermeability. FASEB J. 2008; 22:3728–35. [PubMed: 18606869]
35. Ryan GB, Majno G. Acute inflammation: a review. Am J Pathol. 1977; 86:183–276. [PubMed: 64118]
36. Balsitis SJ, Coloma J, Castro G, et al. Tropism of dengue virus in mice and humans defined by viral nonstructural protein 3-specific immunostaining. Am J Trop Med Hyg. 2009; 80:416–24. [PubMed: 19270292]
37. Kawai T, Akira S. Innate immune recognition of viral infection. Nat Immunol. 2006; 7:131–7. [PubMed: 16424890]
38. Mori M, Rothman AL, Kurane I, et al. High levels of cytokine-producing cells in the lung tissues of patients with fatal hantavirus pulmonary syndrome. J Infect Dis. 1999; 179:295–302. [PubMed: 9878011]
39. Borges AA, Campos GM, Moreli ML, et al. Hantavirus cardiopulmonary syndrome: immune response and pathogenesis. Microbes Infect. 2006; 8:2324–30. [PubMed: 16793309]
40. Minagar A, Long A, Ma T, et al. Interferon (IFN)-beta 1a and IFN-beta 1b block IFN-gamma-induced disintegration of endothelial junction integrity and barrier. Endothelium. 2003; 10:299–307. [PubMed: 14741845]
41. Munoz-Jordan JL, Sanchez-Burgos GG, Laurent-Rolle M, Garcia-Sastre A. Inhibition of interferon signaling by dengue virus. Proc Natl Acad Sci U S A. 2003; 100:14333–8. [PubMed: 14612562]
42. Rath PC, Aggarwal BB. Antiproliferative effects of IFN-alpha correlate with the downregulation of nuclear factor-kappa B in human Burkitt lymphoma Daudi cells. J Interferon Cytokine Res. 2001; 21:523–8. [PubMed: 11506747]
43. Sidky YA, Borden EC. Inhibition of angiogenesis by interferons: effects on tumor- and lymphocyte-induced vascular responses. Cancer Res. 1987; 47:5155–61. [PubMed: 2441862]
44. Nooteboom A, Hendriks T, Otteholler I, van der Linden CJ. Permeability characteristics of human endothelial monolayers seeded on different extracellular matrix proteins. Mediators Inflamm. 2000; 9:235–41. [PubMed: 11200364]
45. Ribatti D, Nico B, Vacca A, Roncali L, Dammacco F. Endothelial cell heterogeneity and organ specificity. J Hematother Stem Cell Res. 2002; 11:81–90. [PubMed: 11847005]
46. Renkonen J, Tynninen O, Hayry P, Paavonen T, Renkonen R. Glycosylation might provide endothelial zip codes for organ-specific leukocyte traffic into inflammatory sites. Am J Pathol. 2002; 161:543–50. [PubMed: 12163379]
47. Harhaj NS, Antonetti DA. Regulation of tight junctions and loss of barrier function in pathophysiology. Int J Biochem Cell Biol. 2004; 36:1206–37. [PubMed: 15109567]
48. Majno G, Palade GE. Studies on inflammation. 1. The effect of histamine and serotonin on vascular permeability: an electron microscopic study. J Biophys Biochem Cytol. 1961; 11:571–605. [PubMed: 14468626]
49. Halstead SB. Dengue. Lancet. 2007; 370:1644–52. [PubMed: 17993365]
50. Ajariyakhajorn C, Mammen MP Jr, Endy TP, et al. Randomized, placebo-controlled trial of nonpegylated and pegylated forms of recombinant human alpha interferon 2a for suppression of dengue virus viremia in rhesus monkeys. Antimicrob Agents Chemother. 2005; 49:4508–14. [PubMed: 16251289]

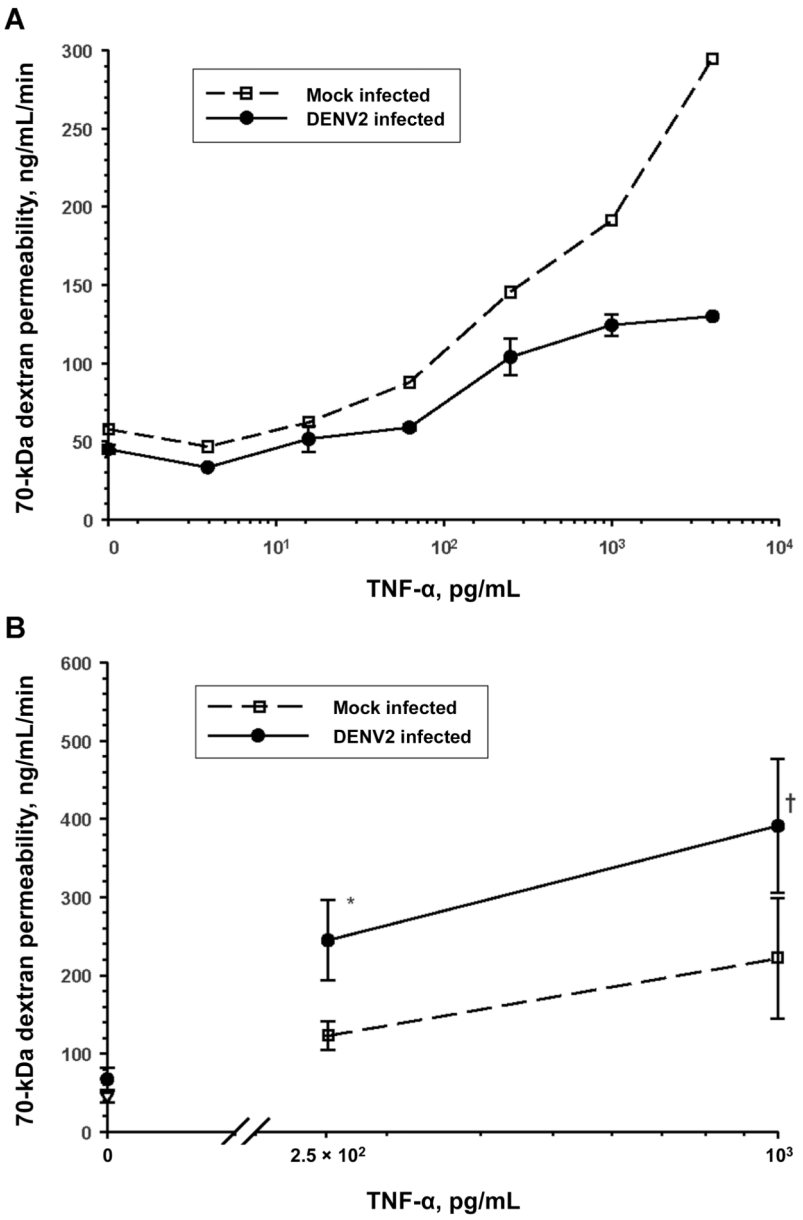

Figure 1.

Differential regulation of tumor necrosis factor (TNF)–*α*–driven hyperpermeability over time by dengue virus type 2 (DENV2) infection (multiplicity of infection, 0.5) of human umbilical vein endothelial cell (HUVEC) monolayers. *A,* Amelioration of TNF-*α*–mediated endothelium hyperpermeability to 70-kDa dextran by DENV2 at 72 h after infection. Data are means ± standard errors from 2 representative experiments. *B,* Augmentation of TNF-*α*–mediated endothelium hyperpermeability to 70-kDa dextran by DENV2 at 7 days after infection (for 250 pg/mL TNF-*α*, $n = 4$; for 1 ng/mL TNF-*α*, $n = 8$). *$P = .10$ for DENV2 infection vs. mock infection ($n = 3$); † $P = .01$ for DENV2 infection vs. mock infection.

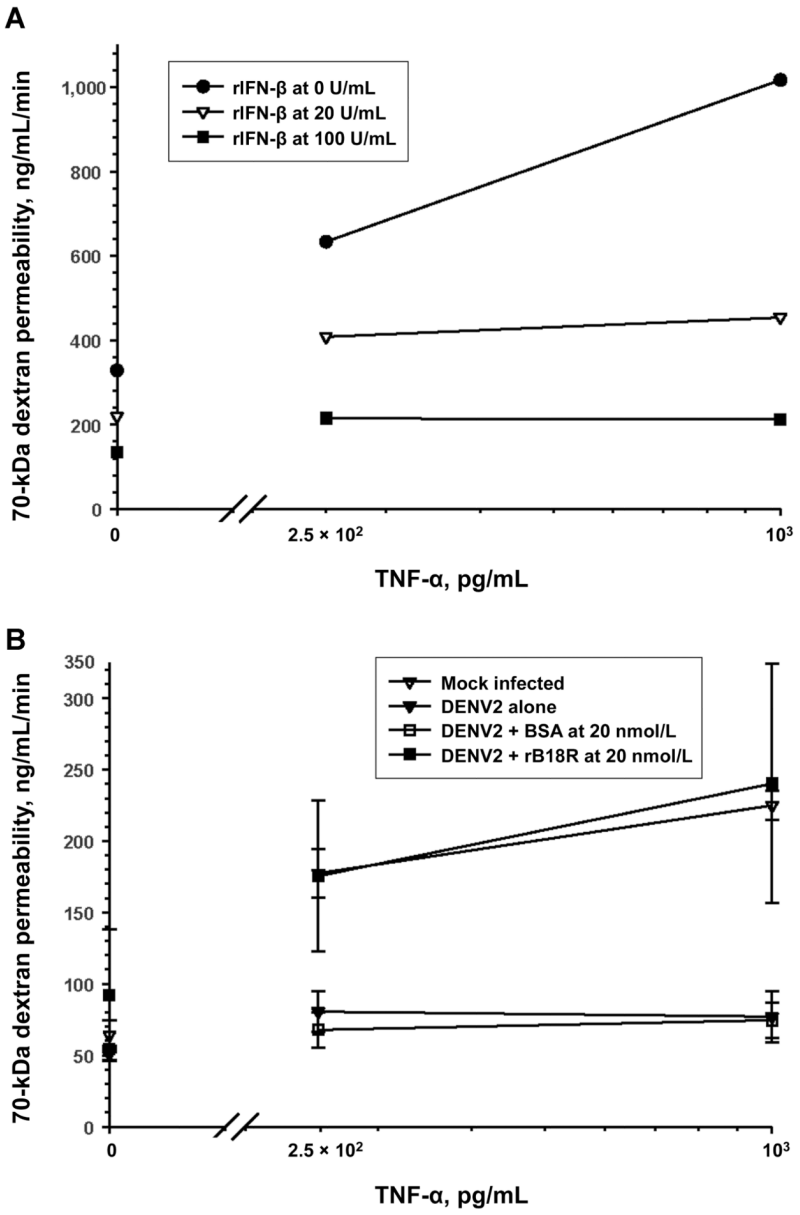

Figure 2.

Suppression of tumor necrosis factor (TNF)–*α*–driven endothelium hyperpermeability and mediation of the early barrier-enhancing effects of dengue virus type 2 (DENV2) infection by type I interferon (IFN). Recombinant (r) TNF-*α*–mediated increases in human umbilical vein endothelial cell (HUVEC) monolayer permeability to 70-kDa dextran were measured 72 h after the addition of rIFN-*β* or DENV2 infection (multiplicity of infection, 0.5) with or without a type I IFN signaling antagonist (rB18R). *A*, Effect of rIFN-*β* on rTNF-*α*–mediated hyperpermeability. *B*, Effect of type I IFN antagonism on the DENV2 suppression of rTNF-*α*–mediated macromolecule permeability. BSA, bovine serum albumin. Data are means ± standard errors from 2 experiments.

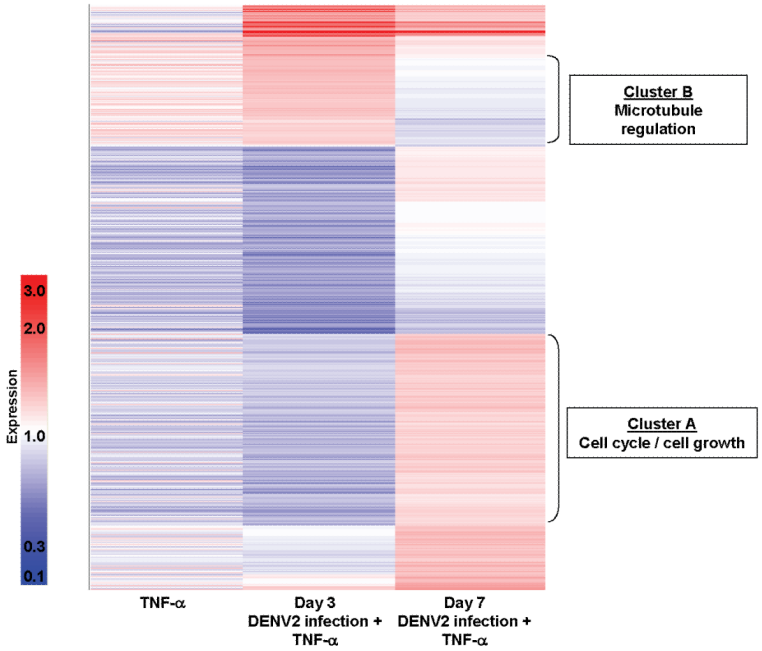

Figure 3.

No enhancement of expression of type I interferon (IFN)–stimulated genes (ISGs) due to tumor necrosis factor (TNF)–*α* stimulation 1 week after dengue virus type 2 (DENV2) infection of human umbilical vein endothelial cells (HUVECs).

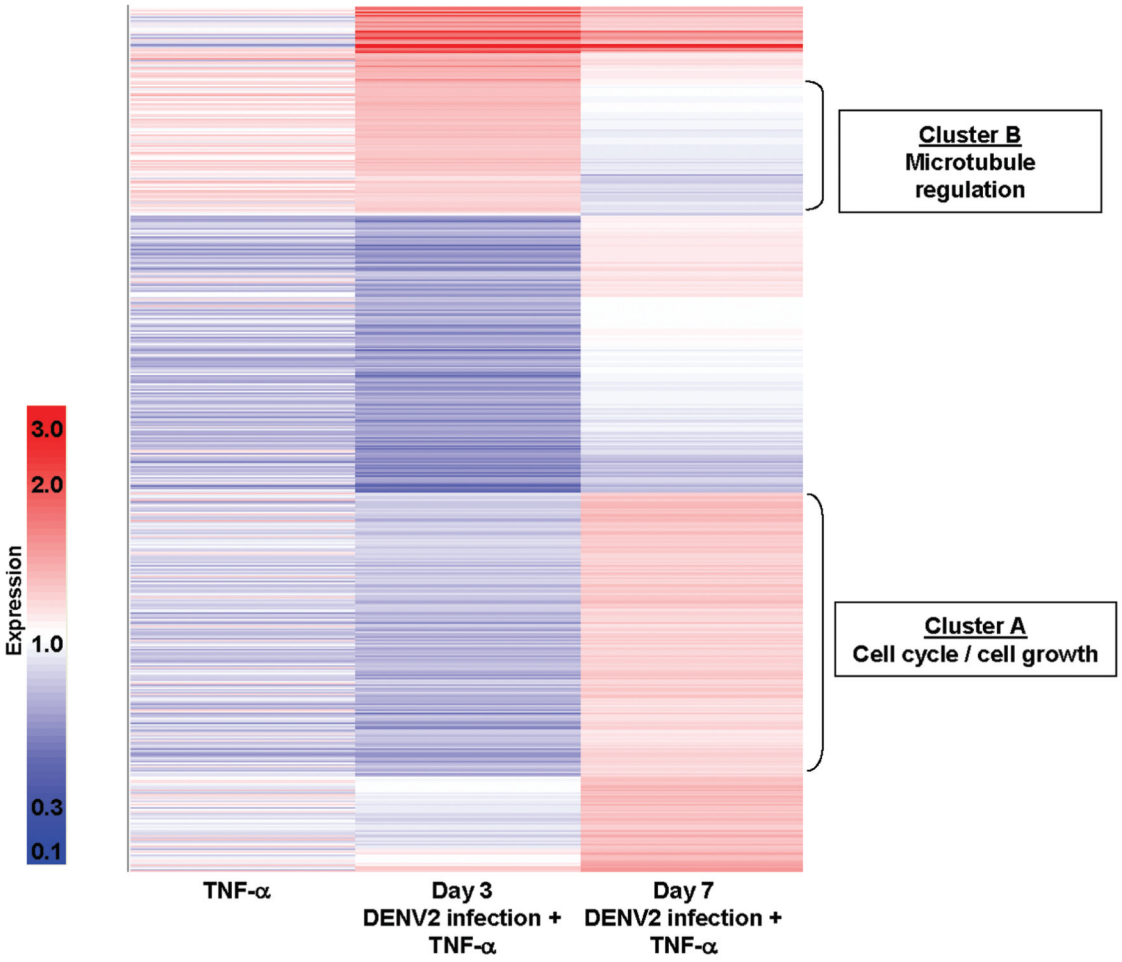

Figure 4.

Differential cellular gene expression in tumor necrosis factor (TNF)–*α*–stimulated human umbilical vein endothelial cells (HUVECs) between days 3 and 7 after dengue virus type 2 (DENV2) infection. Equal amounts of cellular RNA from 4 replicate experiments were pooled for each condition. Affymetrix HG-Focus arrays were used to select the genes that were expressed at levels differing by at least 1.25-fold between days 3 and 7 (a total of 1416 genes). These genes were organized by hierarchical cluster analysis using a Pearson correlation metric. Colors indicate the relative changes in induction (dark red represents 3-fold up-regulation, white represents no change, and dark blue represents 10-fold down-regulation). All signal values are normalized to the mock-infected HUVEC condition. The left column shows mean values for HUVECs stimulated overnight with recombinant (r) TNF-*α* (1 ng/mL) at 3 and 7 days after mock infection. The middle and right columns show the signal values for HUVECs stimulated overnight with rTNF-*α* (1 ng/mL) at 3 and 7 days after DENV2 infection (multiplicity of infection, 0.5), respectively. Gene ontology analysis for the genes contained in clusters A and B was conducted as described in Methods.

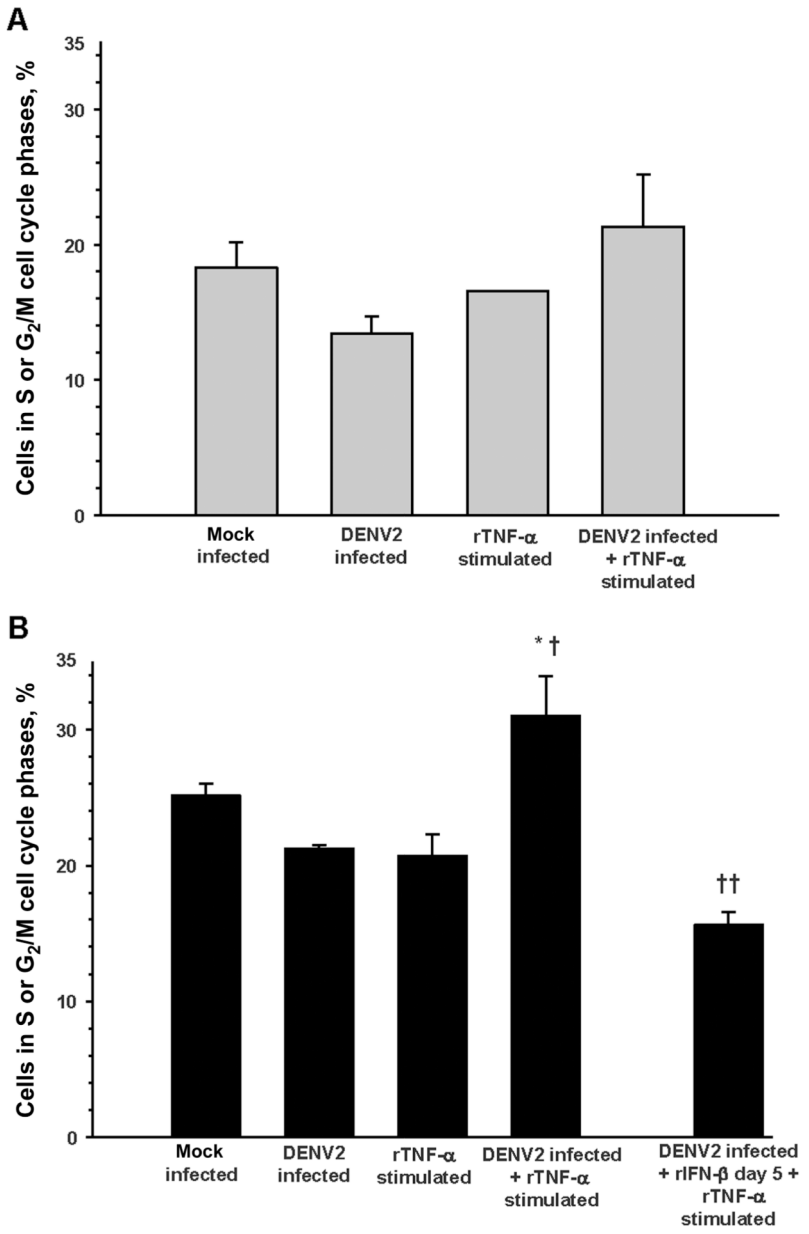

Figure 5.

Augmentation of endothelial cell cycle progression by tumor necrosis factor (TNF)–α stimulation 1 week after dengue virus type 2 (DENV2) infection. Cell cycle phases were determined by propidium iodide staining of cellular DNA content, flow cytometry analysis, and ModFit software modeling. Data are means ± standard errors of independent experiments. *A*, Day 3 conditions: mock infection, DENV2 infection (multiplicity of infection, 0.5), overnight recombinant (r) TNF-α stimulation (1 ng/mL), and DENV2 infection plus overnight rTNF-α stimulation (n = 4 for all; no significant differences between conditions). *B*, Day 7 conditions: mock infection (n = 4), DENV2 infection (multiplicity of infection, 0.5; n = 7), overnight rTNF-α stimulation (1 ng/mL; n = 4), DENV2 infection plus overnight rTNF-α stimulation (n = 7), and DENV2 infection plus 500 U/mL rIFN-β (day 5) plus overnight rTNF-α stimulation (n = 4). *P = .06 for the comparison with mock infection; †P = .01 for the comparisons with DENV2 infection and

with rTNF-α stimulation; ††$P < .001$ for the comparison with DENV2 infection plus rTNF-α stimulation.

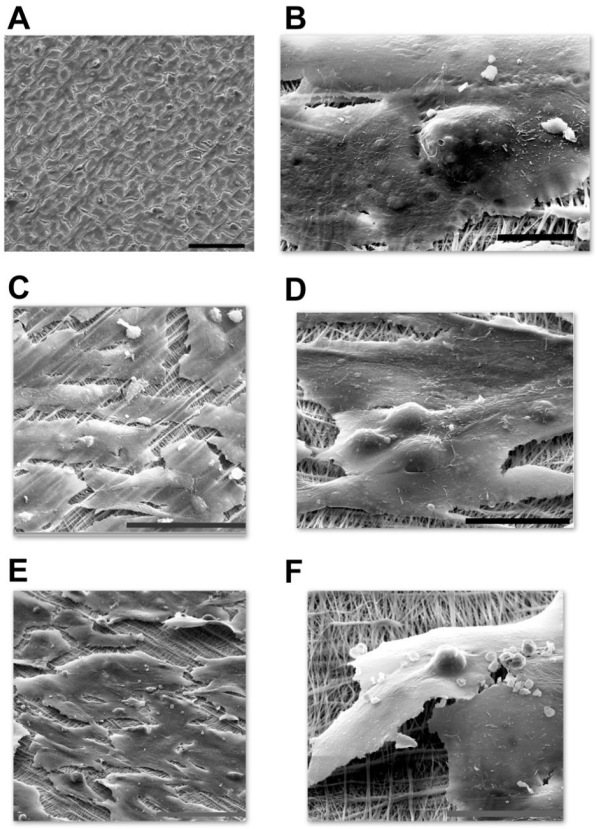

Figure 6.

Scanning electron micrographs of human umbilical vein endothelial cell (HUVEC) monolayers on collagen-coated transwell inserts. Day 3 dengue virus type 2 (DENV2)–infected HUVEC monolayers have a cobblestone appearance (*A;* bar, 100 μm). Day 7 DENV2-infected HUVECs remain flat and are adherent to collagen fibrils and the underlying matrix (*B;* bar, 10 μm). Recombinant tumor necrosis factor (rTNF)–α–stimulated HUVECs (*C;* bar, 100 μm) and day 3 DENV2-infected plus rTNF-α–stimulated HUVECs (*D;* bar, 10 μm) are elongated and are adherent to the underlying matrix. Elongated morphology with detachment is prominent in day 7 DENV2-infected plus rTNF-α–stimulated HUVECs (*E* and *F;* bars, 100 and 30 μm, respectively).

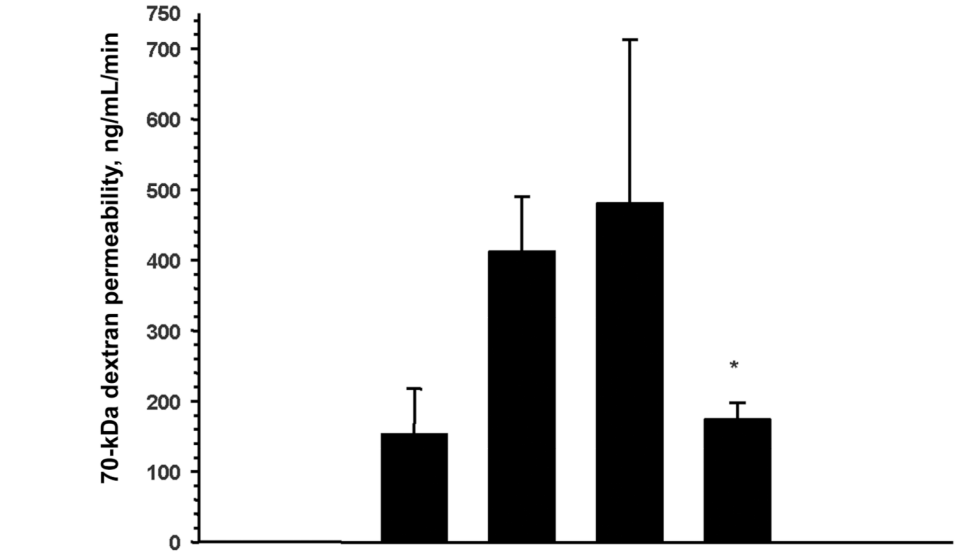

DENV2 at MOI of 0.5 (day 0)	+	+	+	+
Doxycycline at 50 μmol/L (day 4)	-	-	+	-
rIFN-β at 500 U/mL (day 5)	-	-	-	+
rTNF-α at 1 ng/mL (day 6)	-	+	+	+

Figure 7.

Effects of the antiangiogenesis compounds doxycycline and recombinant (r) type I interferon (IFN) on the macromolecule permeability of day 7 dengue virus type 2 (DENV2)–infected plus recombinant (r) tumor necrosis factor (TNF)–α–stimulated human umbilical vein endothelial cell (HUVEC) monolayers. HUVEC monolayer permeability to 70-kDa dextran was measured 7 days after DENV2 infection (multiplicity of infection, 0.5) and after overnight rTNF-α stimulation (1 ng/mL). Doxycycline (50 μmol/L) or rIFN-β (500 U/mL) was added to the cell culture medium before rTNF-α at the indicated time points. Data are means ± standard errors from 4 experiments. *P < .01 for the comparison with DENV2 infection plus rTNF-α stimulation.